Agarose-Assisted Dip-Pen Nanolithography of Oligonucleotides and Proteins

Andrew J. Senesi,[†,#] Dorota I. Rozkiewicz,[‡,#] David N. Reinhoudt,[‡] and Chad A. Mirkin[†,*]

[†]Department of Chemistry and International Institute for Nanotechnology, Northwestern University, 2145 Sheridan Road, Evanston, Illinois 60208-3113, and [‡]Laboratory of Supramolecular Chemistry and Technology, MESA+ Institute for Nanotechnology, University of Twente, P.O. Box 217, 7500 AE Enschede, Netherlands. [#]These authors contributed equally to this work.

ABSTRACT This paper describes a method for the direct transfer of biomolecules encapsulated within a viscous fluid matrix by dip-pen nanolithography (DPN). The method relies on the use of agarose as a "universal" carrier that is compatible with many types of biomolecules including proteins and oligonucleotides. Agarose-assisted DPN allows one to generate nanoarrays of such materials on activated glass substrates with the same deposition rates for different biomolecules, which will greatly expand future capabilities for parallel, multiplexed biomolecule deposition. The fluidity of the matrix may be systematically varied to control the deposition process, resulting in an additional parameter affecting deposition rates besides tip-substrate contact-time and humidity. Agarose-assisted DPN results in extremely fast biomolecule patterning with typical contact times less than 1 s. Feature sizes as small as 50 nm are demonstrated. The biorecognition properties of both protein and oligonucleotide structures are characterized by studying their reactivity with fluorophore-labeled antibody and complementary oligonucleotide sequences, respectively.

KEYWORDS: dip-pen nanolithography · matrix-assisted deposition · agarose · DNA arrays · protein arrays · scanning probe lithography · atomic force microscopy

Biological microarray technology has led to significant advances in biology, biochemistry, and medicine. These arrays form the cornerstone of modern genomics and proteomics, with many applications in gene profiling,[1] protein screening,[2] and drug discovery.[3] In their current formats, spot diameters typically range from 1 to 150 μm. Recent studies have focused on decreasing feature size because high density biomolecule arrays allow one to extract more information per unit area, increase sensitivity, and use smaller sample volumes.[4] In addition, with nanoscale features, one can essentially place an entire array underneath a single cell and probe both monovalent and multivalent cell−surface interactions.[5] Also, with nanoscale features, one can manipulate individual biological constructs such as viruses[6] and perhaps even proteins at the single particle level. In all of these applications, facile signal quantification requires homogeneity in both feature size and the density of biomolecules within an array. Consequently, it is necessary to achieve this feature size reduction while maintaining the ability to create homogeneous spots for each biomolecule within and between arrays.

A variety of methods have been used to deposit DNA and proteins on surfaces with nanoscale resolution.[4] These include several types of scanning probe lithography,[7−11] e-beam lithography,[12] nanocontact printing,[13] and nanoimprint lithography.[14] One tool that is particularly attractive in this regard is the scanning probe technique known as dip-pen nanolithography[15−17] (DPN). DPN has sub-50 nm resolution, is soft matter-compatible, and has the registration requirements to make high quality arrays of biological molecules. In addition, in combination with both 1-dimensional (1-D) and 2-dimensional (2-D) cantilever arrays and the related scanning probe contact printing technique, polymer pen lithography (PPL), DPN has recently been transformed from a serial into a massively parallel method, with as many as 11 million pens drawing nanostructures at a rate of ~7 trillion features per minute.[18]

There are several challenges associated with using direct-write scanning probe techniques such as DPN in the large-scale parallel generation of biological arrays. The first involves transport, and specifically, ways to facilitate the movement of large macromolecules from the surface of an AFM tip to the substrate one intends to pattern. To solve this problem, many strategies have been attempted with varying degrees of success. These include tip modification procedures that change the adhesion properties of the tip for biomolecules,[7−10] the use of specialty substrates such as Ni with his-

*Address correspondence to chadnano@northwestern.edu.

Received for review June 4, 2009 and accepted July 16, 2009.

Published online July 31, 2009.
10.1021/nn9005945 CCC: $40.75

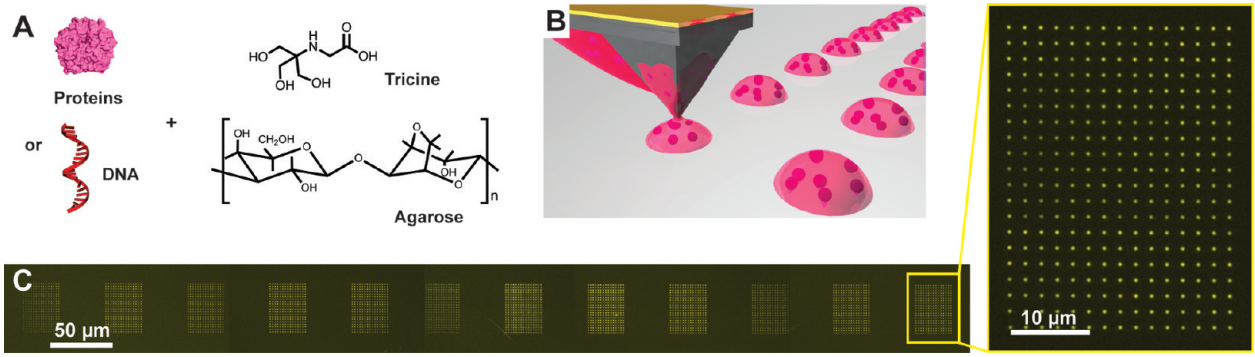

Figure 1. (A) A schematic representation of ink and matrix components; (B) an illustration showing the process of agarose-assisted DPN; (C) epifluorescent microscope image of a 15 × 20 array of 500 nm Cy3 labeled oligonucleotide features generated in parallel from a 12-tip cantilever array.

tagged ink moieties, and nanopipettes with ink-transport facilitated by capillary action.[19] Indirect patterning methods have been explored to circumvent the issue of directly transporting high molecular weight species.[5,20,21] However, direct write techniques are preferable, resulting in decreased cross contamination between biological entities during multiplexed deposition.

The second challenge pertains to the differences in diffusion properties for different molecules. With one molecule type, tip-substrate contact-time and humidity are typically used to control transport rates. These parameters are very effective in the context of generating single ink structures. However, with a combinatorial library of biomolecules, each ink will have a different set of diffusion and adhesion properties. Therefore, the challenge of simultaneously transporting many different molecules with control over feature size is daunting in the context of a conventional DPN experiment.

The third challenge pertains to bioactivity. One must develop ways of transporting the desired molecules in such a way that they maintain their biorecognition properties. A single, general method for patterning different types of biomolecules that enables direct transport to the surface while preserving their biological activity would be highly desirable for large scale parallel generation of biomolecule arrays.

Herein, we describe the use of agarose as a universal carrier matrix to deposit proteins and DNA, the two most important classes of biomolecules, on a substrate with nanoscale resolution. The transfer of a matrix along with the analyte during DPN patterning has been observed by our group,[9] and also Bao,[22] and Lenhert.[23] Nevertheless, to the best of

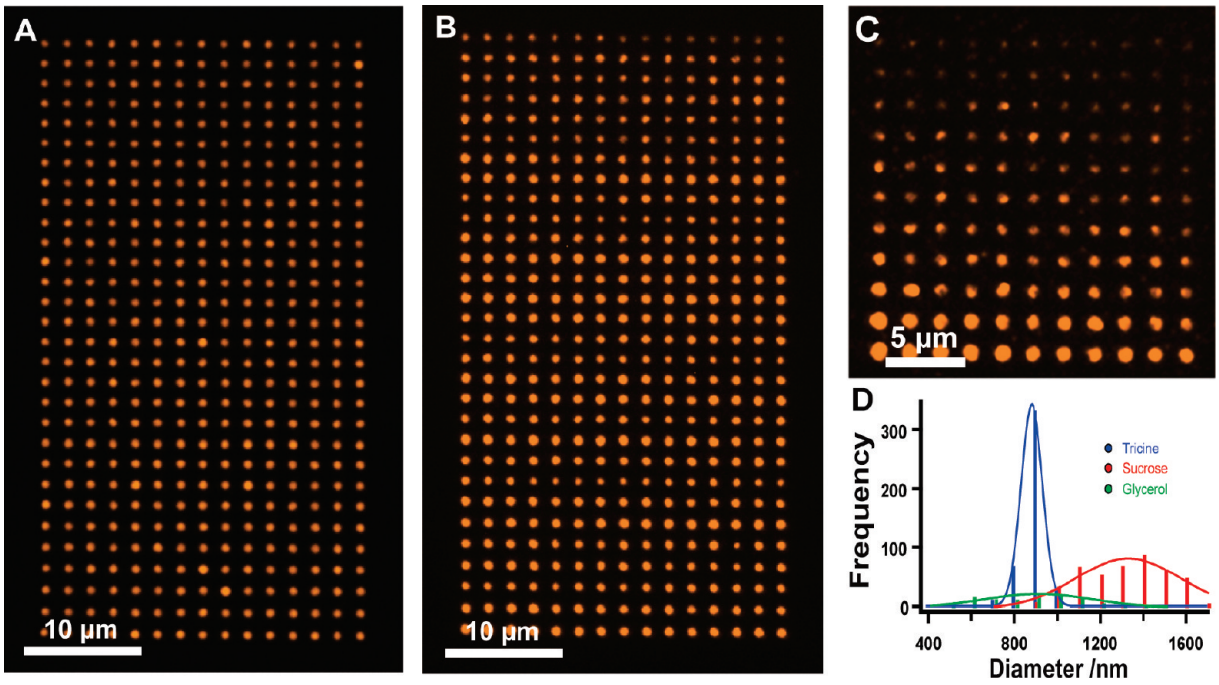

Figure 2. Fluorescence microscope image of CTβ deposited by agarose assisted DPN using (A) tricine, (B) sucrose, and (C) glycerol as accelerating agents. In each array, features were patterned beginning with the lower left and moving right, then up to the next row and left, in a snake-like pattern. (D) Histogram of spots patterned in panels A, B, and C.

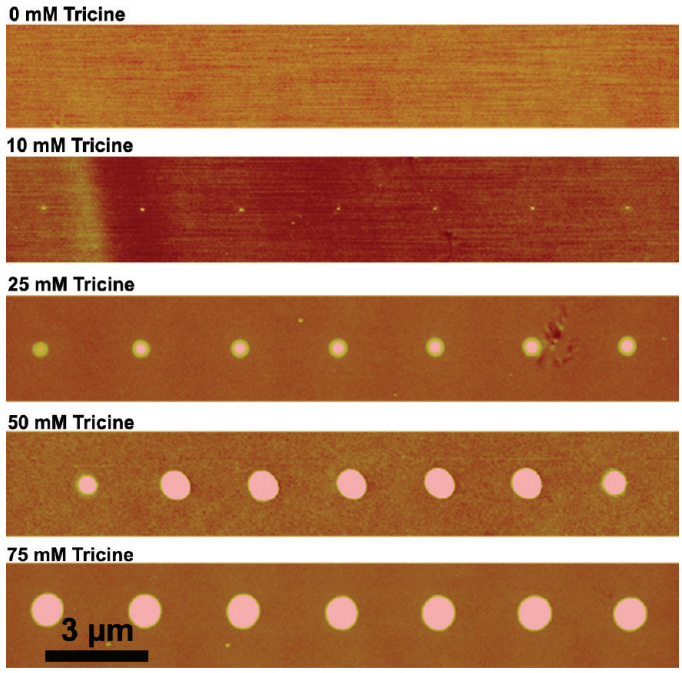

Figure 3. Spots generated by agarose-assisted DPN with increasing tricine concentration from 0−75 mM at 0.5 s dwell time and 50% humidity.

our knowledge this is the first report where the composition of the matrix may be systematically adjusted to control deposition.

Agarose is a linear biocompatible polysaccharide, composed of alternating (1−3)-linked β-D-galactose and (1−4)-linked (3−6)-anhydro-α-L-galactose that becomes a thermo-reversible hydrogel when heated in water.[24,25] It has been used extensively in biology as a stabilizer and support for many types of biomolecules[26,27] and may be fashioned into a stamp for contact printing.[28,29] In the work described herein, however, the agarose gel is not only used as a stabilizer but also as a carrier, where it is transferred as a matrix with the desired biomolecule to a substrate in the context of a DPN experiment. The use of agarose as a carrier ink has several advantages over the direct deposition of a pure biomolecule sample for use in a DPN experiment. First, the hydrogel stabilizes and protects proteins from drying and denaturing while on the tip. Second, the increased viscosity compared to a buffered solution and the partially hydrophobic nature of the fluid gel facilitates ink adsorption on the AFM tip without prior surface modification, a requirement of several previous protocols for effecting protein adsorption and subsequent transport.[8,9] Third, the fluidity of the gel may be systematically varied by controlling the concentration of agarose in addition to chemical additives (e.g., tricine buffer), providing a third parameter effecting deposition rates besides the traditional tip-substrate contact-time and humidity used in DPN.

RESULTS AND DISCUSSION

Our strategy for agarose-assisted DPN begins first with the preparation of an aqueous matrix composed of 0.15% agarose and an "accelerator" species containing hydroxyl, amine, or carboxylic acid functional groups used to control gel fluidity. After briefly heating until the agarose completely dissolves, proteins (0.5 mg/mL final concentration) or DNA (50 μM final concentration) is added (Figure 1A). Control over deposition parameters was examined for two model proteins, cholera toxin β subunit (CTβ) labeled with Alexa Fluor 594 and a fluorescein-labeled rabbit antigoat IgG antibody and a 3′ heptyl amine modified oligonucleotide possessing a 5′ Cy3 label. Codelink *N*-hydroxysuccinimide-ester activated substrates were used to covalently immobilize the amine-modified oligonucleotides and proteins (through their exterior amine groups) by the formation of amide linkages. Significantly, the agarose matrix may be washed away, leaving only biomolecules covalently bonded to the substrate (Supporting Information). A schematic representation of the DPN process is shown in Figure 1B. By control over humidity, tip-substrate contact time, and gel fluidity, spots of either DNA or proteins are patterned in parallel with nanoscale resolution (Figure 1C).

All DPN experiments were performed within a feedback controlled humidity chamber, which allowed for control of relative humidity between ~10 to 95%. Without addition of an accelerator such as tricine to the agarose matrix, agarose transport with or without DNA or proteins did not occur on hydrophilic Codelink substrates up to 90% relative humidity. Above 90% relative humidity, agarose patterns could be imaged by AFM, though patterning was not reproducible, spatial resolution was poor, and epifluorescence microscopy indicated no significant transfer of biomolecules. A systematic study of other typical DPN parameters such as contact-time and tip speed did not further improve patterning. Furthermore, the proteins by themselves inked from a carboxylic acid functionalized AFM tip[8] would not transport from the tip to substrate surface.

The addition of a molecule possessing a hydroxyl, amine, or carboxylic acid functional group capable of hydrogen bonding with the agarose matrix during ink preparation facilitated transport during agarose-assisted DPN. These classes of molecules were chosen as "accelerators" because of their known ability to interact with the agarose matrix *via* hydrogen bonding as well as decrease the availability of water necessary for stabilization of the gel network. This, in turn, modulates the viscoelastic properties of the gels by impeding the interstrand bundling and the transformation of agarose helices into coils.[30−34] Tricine, tris (1,1,1-hydroxymethyl) aminomethane (tris), tris (1,1,1-hydroxymethyl) ethane (THME), glycerol, sucrose, and

ethylenediaminetetraacetic acid (EDTA) all accelerate the deposition rates for agarose-assisted DPN. In general, when progressing from the triol THME to tris (by incorporation of an amine functional group), to tricine, (which in addition included a carboxylic acid functional group), deposition rates increased for a given accelerator concentration (data not shown). Thus, THME concentrations of 250−500 mM provide similar accelerating effects as tris at the 100−300 mM range, and tricine at the 10−75 mM range. With four carboxylic acid functional groups, EDTA provided the greatest accelerating effects, performing comparably to those above at concentrations of 1−30 mM. Conversely, sodium chloride provided no ability to accelerate deposition rates up to 1 M concentration. Both tris and EDTA were discarded as potential accelerators for agarose-assisted DPN, as tris contains a primary amine, which is incompatible with amine-based immobilization strategies, whereas EDTA is known to sequester metal ions from proteins, affecting their biological activity.

Tricine, sucrose, and glycerol were further examined as accelerating agents for agarose-assisted DPN according to two conditions, the ability to generate large-scale arrays and form homogeneous features within an array. Three AFM tips were coated with one of the three different agarose/accelerator matrices, also including CTβ, and used for DPN experiments at 50% humidity (Figure 2). Arrays of 450 spots were generated for matrix inks that included tricine and sucrose, and an array of 121 spots was generated for the glycerol matrix ink. Each array was subsequently analyzed by fluorescence microscopy. Tricine provided the best results for creating large-scale arrays with homogeneous distribution. When sucrose was used as the accelerating entity, inhomogeneous feature sizes, varying in diameter by 50%, were obtained. For glycerol, the feature size decreased by ~60% over the array, with feature size progressively decreasing with each additional spot.

The feature sizes obtained from agarose-assisted DPN could be controlled by adjusting tricine concentration. As a proof of concept, a series of seven dots was patterned with a 0.5 s contact time for a CTβ matrix ink with tricine concentrations ranging from 0−75 mM at 50% humidity (Figure 3). Spot sizes increased from 0 (*i.e.*, no deposition at 0 mM tricine) to 111 ± 10, 555 ± 32, 869 ± 83, and 962 ± 79 nm for 10, 25, 50, and 75 mM tricine, respectively. This increase in feature size occurs for two reasons. First, the tricine is partially hygroscopic, causing moisture to be extracted from the air to keep the gel hydrated thus maintaining gel fluidity compared to a matrix without tricine (Supporting Information). Second, the additives themselves interact with the agarose matrix *via* hydrogen bonding, modifying the viscoelastic properties of the gel[30−32] and allowing it to flow more easily from the tip to the substrate (Supporting Information).

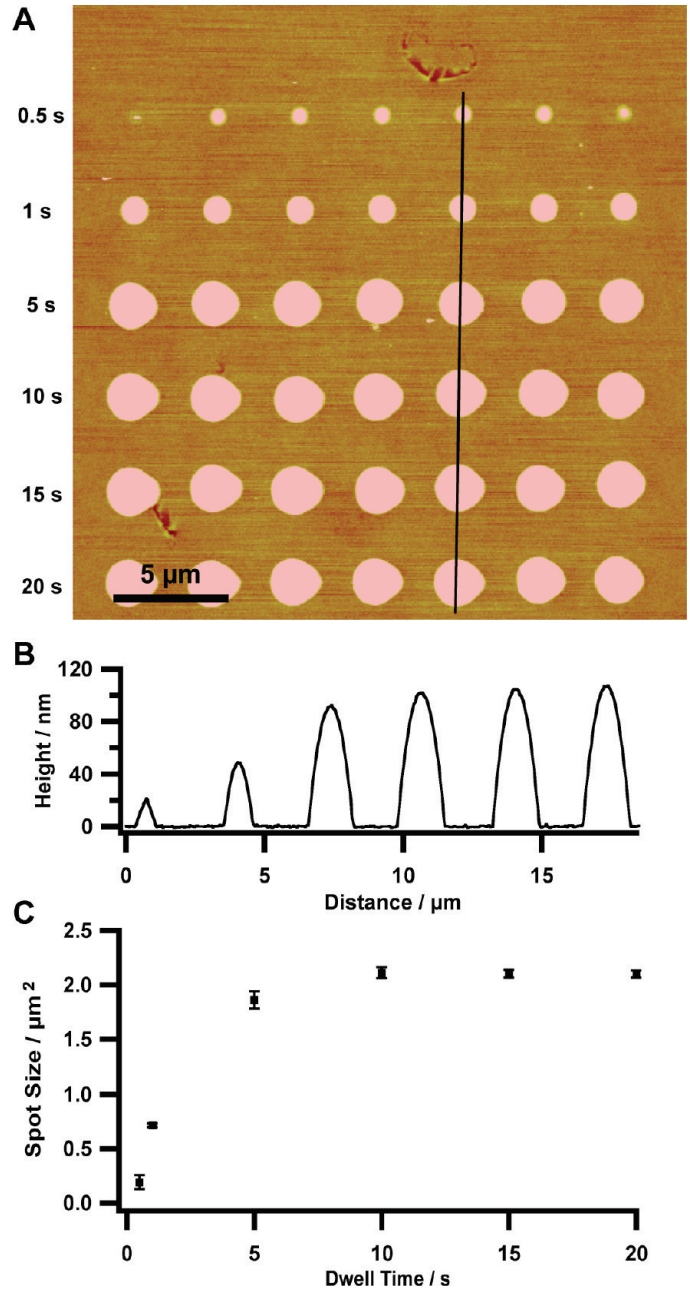

Figure 4. A typical experiment showing saturation behavior for the deposition of antigoat IgG by agarose-assisted DPN with a 10 mM tricine concentration. (A) Tapping-mode AFM image of agarose IgG spots created with 0.5−20 s contact-time. (B) Height profile for spots from panel A. (C) Plot of dwell time *vs* spot size for the same experiment as in panel A. Note that the deposition process begins to saturate both laterally and vertically after approximately 5 s dwell time.

The deposition process was further examined by varying both tricine and tip-substrate contact time. In a typical experiment, the contact-time between an agarose/tricine/biomolecule-coated AFM tip and substrate was varied and subsequently scanned by tapping mode AFM to determine feature size (Figure 4A). For long dwell times up to 20 s, the deposition process displayed limiting behavior (Figure 4 B,C), in contrast to previous studies of alkanethiols on a gold surface.[15,35] Whereas conventional DPN of al-

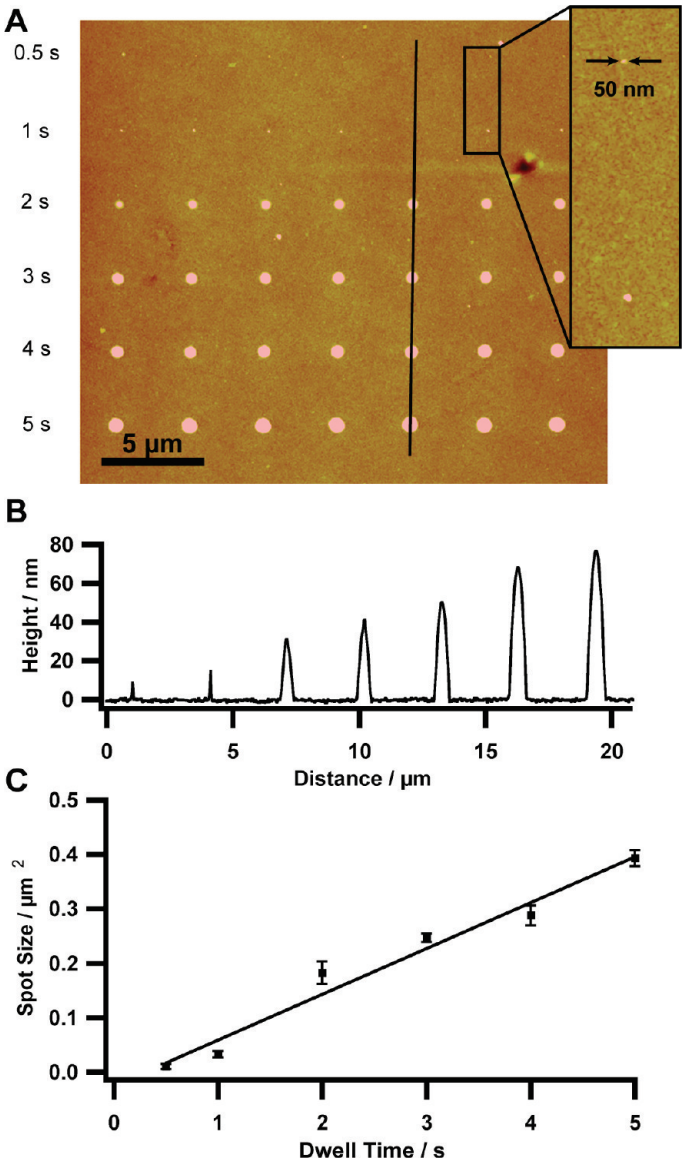

Figure 5. (A) A typical experiment showing the deposition characteristics of agarose-assisted DPN of CTβ with 10 mM tricine by tapping-mode AFM for dwell times ranging from 0.5 −5 s. The minimum feature size is 50 nm for 0.5 s dwell time. (B) Height profile for the AFM image in panel A. (C) Spot size as a function of dwell time from the AFM data in panel A showing that agarose-assisted DPN displays typical linear deposition characteristics for short dwell times.

kanethiols takes advantage of a water meniscus to facilitate the transport of a dry ink to the surface, the agarose matrix is deposited as a wet gel. Further, alkanethiols chemisorb to a gold substrate, as opposed to the agarose matrix, which interacts with the surface via physisorption. This behavior of liquid spotting by DPN has been recently observed for the DPN deposition of a wet solution of Ag nanoparticles in glycerol.[36] Similarly, the agarose ink deposition reached a point where feature size did not increase with increasing tip-substrate contact-time.

For short dwell times, generally less than 5 s, however, the deposition process may be modeled with a linear increase in spot area for increasing dwell times (Figure 5), predicted theoretically[37] and observed experimentally for materials ranging from alkanethiols[35] and silazanes[38] to oligonucleotides[7] and salts.[20] The dwell time at which the deposition process switched between linear and nonlinear behavior generally decreased for increasing tricine concentrations, although it was partly dependent on inking conditions. For a 10 mM tricine concentration, a linear deposition process was typically observed up to ~5 s contact time, while linear deposition resulted for up to 1 s for 75 mM tricine concentration.

We hypothesized that the fluidity of the agarose matrix ink would be the dominant factor in determining transport rates, resulting in identical feature sizes for different biomolecules deposited by agarose-assisted DPN. To prove the same deposition rate could be obtained for two separate agarose matrix protein inks given identical tip morphology and inking conditions, a single tip was used to pattern both proteins, each inked from the same inkwell channel. Interestingly, these proteins could not be deposited by previously reported DPN procedures on Codelink substrates.[8] The tip was first conditioned by inking with a 10 mM tricine, CTβ agarose matrix. The tip was washed in DI water for 1 min and re-inked with the same agarose matrix, and the deposition rate was examined at 60% relative humidity by varying contact-time with subsequent imaging by tapping mode AFM. The same tip was again washed in DI water for 1 min, inked with a 10 mM tricine antigoat IgG agarose ink, and again used to determine the deposition rate at 60% relative humidity (Figure 6). Within experimental error, both protein inks exhibit nearly identical spot sizes for each dwell time and show deposition rates of 0.94 $\mu m \cdot s^{-1}$. This is a significant observation, as proteins often transport at different rates as a function of size and chemical makeup.

Using agarose-assisted DPN, it is possible to pattern nanoscale protein features at extremely fast rates. Typical deposition rates were on the order of 1 $\mu m^2 \cdot s^{-1}$, which is an order of magnitude greater than the fastest observed diffusion rates of MHA on gold[35] and 1−3 orders of magnitude greater than rates previously observed for proteins[8] or oligonucleotides.[7] By setting a dwell time of 10 ms (the shortest time allowed by our instrument), it was possible to make an arrays of 450 features in approximately 1 min. In fact, the time to move between features took longer than the combined tip-substrate contact-time.

The biological activity and specificity as well as verification of immobilization on the functionalized surface were verified by epifluorescence microscopy for both protein and oligonucleotide arrays. A 15 × 30 dot array of Alexa Fluor 594 labeled CTβ proteins was generated by agarose-assisted DPN from 10 mM tricine agarose matrix (Figure 7a). On the same substrate, a

second array of antigoat IgG antibodies was patterned as a control (Figure 7a). The proteins were allowed to react with the surface for 4 h and then washed with PBS buffer to remove the matrix, leaving biomolecules covalently immobilized on the surface. Significantly, after washing, no matrix could be detected by AFM (Supporting Information). After passivation with an amine-terminated polyethylene glycol to prevent nonspecific adsorption, the protein patterned substrate was challenged with an Alexa Fluor 488-labeled anticholera toxin antibody for 30 min at room temperature. After washing, the substrate was blown dry with N_2 and imaged by epifluorecent microscopy. Figure 7b clearly indicates antibody-antigen binding between anticholera toxin to the CTβ arrays with a signal-to-noise of 2:1 (Figure 8b), while the antigoat IgG provides a negative control with minimal cross reactivity.

Similarly, an array of Cy3-labeled oligonucleotides was generated by agarose-assisted DPN employing 10 mM tricine concentration (Figure 7c). Simultaneously, a negative control random sequence was spotted at a different location on the same substrate by agarose-assisted DPN. After the oligonucleotides had reacted with the surface, the substrate was passivated with ethanolamine and subsequently immersed in a 1 μM aqueous buffered solution (60 mM trisodium citrate, 600 mM NaCl) of a Cy5-labeled probe sequence at 45 °C overnight. Excess probes were removed by washing under vigorous agitation and the substrate was blown dry with N_2. Upon imaging, it is clear that the probe sequence binds its target with signal-to-noise ratios greater than 2:1 at, and only at, the locations of the complementary sequence (Figure 7D). From a technical standpoint, agarose-assisted DPN allows for protein patterning at ambient humidity; it is unnecessary to use a relative humidity upward of 80% to both affect protein deposition and maintain biological activity as was necessary in several previous studies.[8,9] This results in decreased wear on the piezo elements of the AFM.

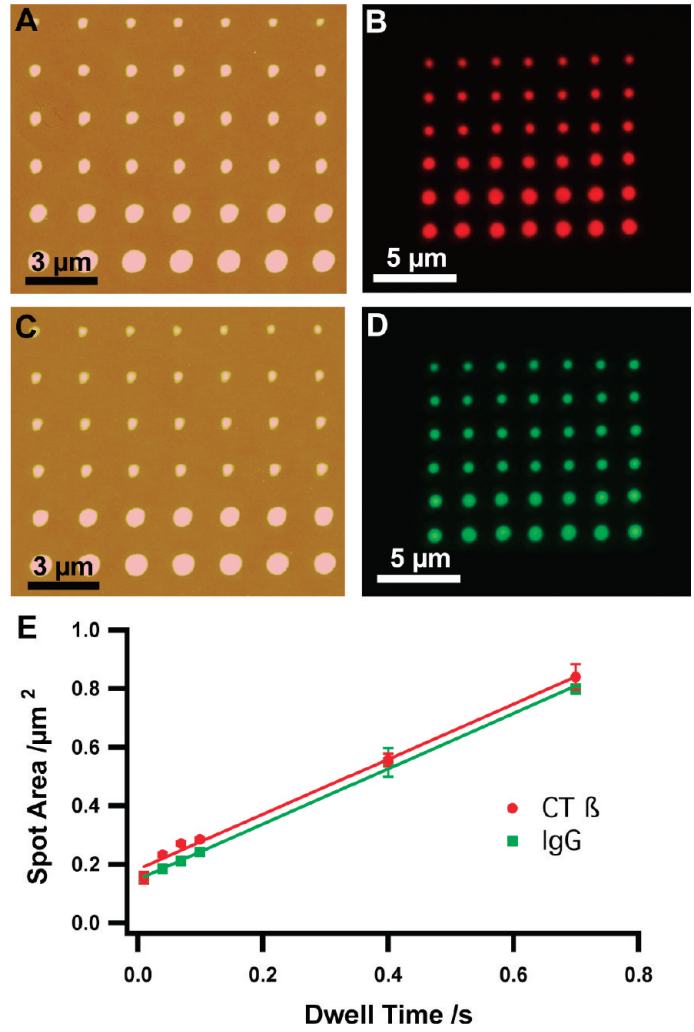

Figure 6. Tapping mode AFM images, (A, C) and epifluorescent images (B, D) of CTβ and IgG, respectively, deposited from the same tip using agarose-assisted DPN. Note that cross contamination of IgG with CTβ during the second inking process cannot be observed by epifluorescent microscopy. (E) Plot of spot size *vs* dwell time for each ink as determined by the AFM images in panel A and C. Given consistent tip morphology and inking conditions, agarose-assisted DPN may be used to pattern multiple proteins with the same feature sizes for the same dwell times.

CONCLUSIONS

In this work we have shown agarose to be an effective matrix to control the deposition process of biomolecules by DPN. The deposition rate may be systematically varied between 0 and 1.5 $\mu m^2 \cdot s^{-1}$ by controlling the concentration of an accelerator such as tricine buffer within the matrix. This provides a third handle to control deposition in addition to the traditional tip-substrate contact-time and humidity used in conventional DPN. Importantly, one can use the agarose and an appropriate amount of accelerator to modulate the rate of protein/matrix transport so that one can realize similar feature sizes from proteins that normally do not transport or transport at different rates in the absence of the accelerators. The agarose matrix may be easily washed away, leaving either proteins or oligonucleotides covalently bonded to the substrate. Though uniformity in terms of tip morphology, array linearity, and inking remain challenging, improvements in methodology of fabricating tip arrays[18] combined with more uniform inking methods[35] will allow for parallel multiplexed biomolecule deposition, each with the same spot size for facile comparison of signal intensity. Significantly, these biomolecules retain activity once attached to the surface, and extreme care need not be used to keep proteins from denaturing on the tip surface. Agarose-assisted DPN is an extremely quick patterning method with deposition rates up to 3 orders of magnitude faster than previously reported printing of biomolecules, which overall decreases time and costs for printing nanoscale biomolecule features by DPN.

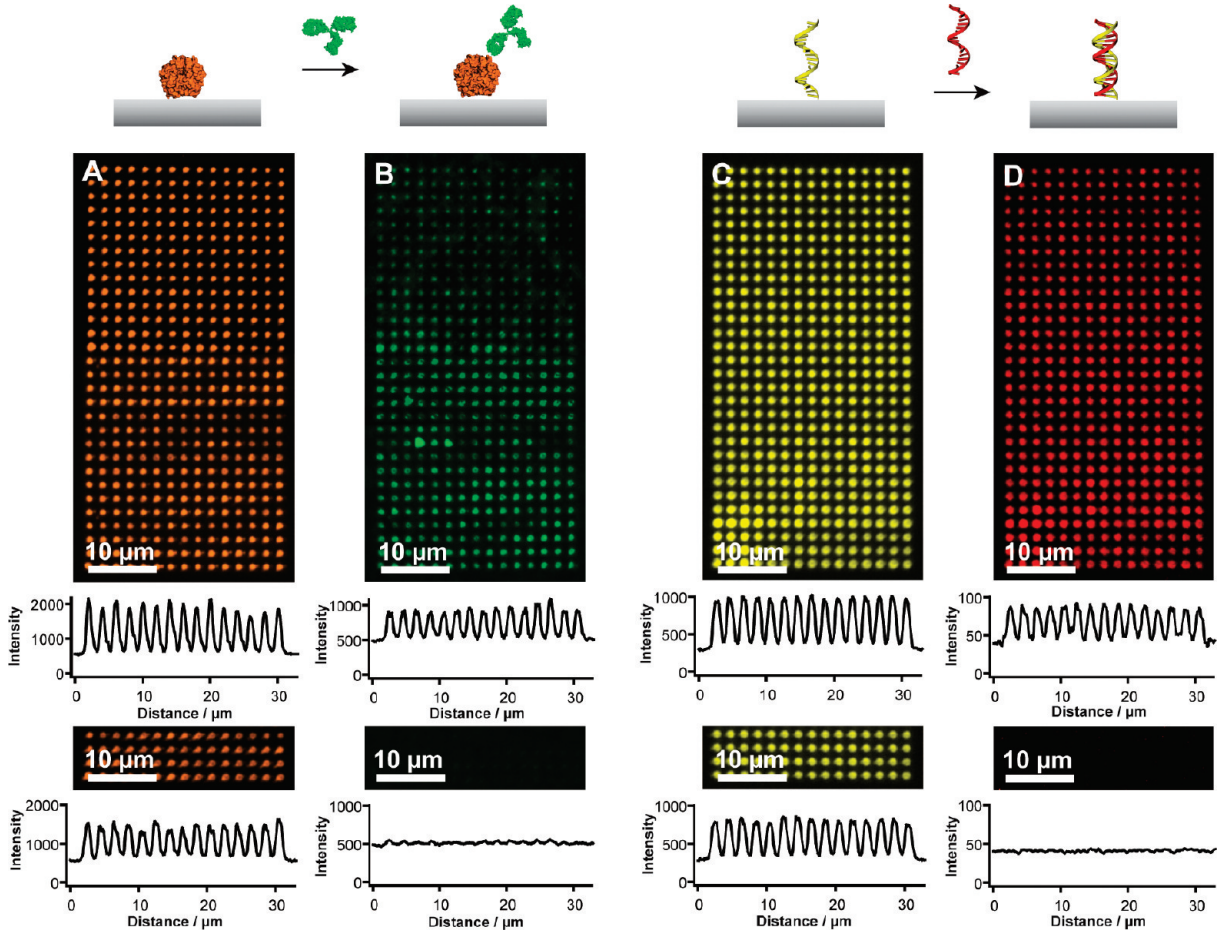

Figure 7. Simultaneous imaging before and after protein antigen binding (A and B) and hybridization (C and D) with negative controls. Alexa Fluor 594 labeled CTβ spotted by agarose-assisted DPN (A upper image) used for antigen binding and Alexa Fluor 594 labeled antigoat IgG (A bottom image) used as a negative control. (B) After probing with Alexa Fluor 488-labeled anticholera toxin showing antigen binding (upper panel) and negative control (lower panel). (C) Cy3-labeled amine modified oligonucleotides with a complementary sequence (upper panel) and a Cy3 labeled amine modified random sequence (lower panel). (D) After hybridization with complementary probe showing hybridization (upper panel) and negative control (lower panel).

Utilizing massively parallel 2-D tip arrays it should be possible to print nanoscale biomolecule dots at rates of 50 million features per min with densities of 25 million spots per cm^2.

EXPERIMENTAL METHODS

Materials. Oligonucleotides were synthesized on an ABI Expidite nucleic acid synthesizer using standard phosphoramidite chemistry[39] with reagents obtained from Glen Research Corporation (Sterling VA). All oligonucleotides were purified *via* reverse phase HPLC on a Varian Prostar 210 HLPC eluted from a Varian Dynamax reverse phase C18 column (Varian, Inc., Walnut Creek, CA) with a 3 mL/min flow rate from a gradient of acetonitrile and triethylammonium acetate. The target sequence employed for DPN studies had the sequence 5′-Cy3-GTG CAC CTG ACT CCT GTG GAG-T_{12}-$(CH_2)_7$-NH_2-3′. The probe sequence was 5′-Cy5-CTC CAC AGG AGT CAG GTG CAC-3′. The random control sequence was 5′-Cy3-TCA TAG TGT GGA CCC CTA GCA-T_{12}-$(CH_2)_7$-NH_2-3′. Alexa Fluor 594-labeled cholera toxin β subunit and Alexa Fluor 594-labeled antigoat IgG were obtained from Molecular Probes Invitrogen. Mouse anticholera toxin IgG1 antibodies were purchased from Biodesign International and labeled with Alexa Fluor 488 (Molecular Probes Invitrogen). Tricine, glycerol, Tris (hydroxymethyl) amine (Tris), ethylenediaminetetraacetic acid (EDTA), Tris (hydroxymethyl) ethane (THME), sucrose, sodium phosphate (Na_2PO_4 and $NaHPO_3$), sodium chloride (NaCl), ethanolamine, and polyethyleneglycol amine (PEG-NH_2, MW 3000) were purchased from Sigma Aldrich (Milwaukee, WI) and used as received. Agarose, low melting temperature (BP165−25), was purchased from Fisher Scientific (Fair Lawn, NJ) and used as received. Codelink activated glass slides were obtained from GE Healthcare (Piscataway, NJ), cut to size, and stored desicated. All buffers and biomolecule solutions were prepared using 18.2 MΩ · cm nanopure water (Barnstead Int., Dubuque, IA). AFM 12-tip M-type cantilever arrays (nominal spring constant 0.5 N/m) and inkwells were purchased from NanoInk, Inc. (Skokie, IL).

Ink Preparation. A 0.3% (w/w) agarose gel was prepared by dissolving agarose in water or a solution containing "accelerating agents" (e.g., tricine buffer, pH 8) by heating for 2 min in a microwave oven. The gel in sol form was mixed with a solution of 50 μM DNA or 1 mg/mL proteins in a 1:1 ratio and incubated at 4 °C for 30 min to ensure matrix formation.

Dip-Pen Nanolithography. DPN was preformed on an NSCRIPTOR DPN platform (NanoInk, Inc., Skokie, IL) in contact mode with the tip lift function enabled for movement between features. All lithography was preformed within a feedback controlled humidity chamber at 50−60% relative humidity. Tips were inked from M-type inkwells by dipping for 5 s. Contact time typically varied between 0.01−20 s.

Surface Antigen Binding. Agarose protein patterns on Codelink slides were allowed to react a minimum of 4 h at 50% humidity

and then washed with PBS (5 min) under vigorous agitation and rinsed with water to remove residual agarose. These substrates were subsequently passivated with PEG-NH_2 1 mg/mL borate buffer pH p for 1 h at room temperature to prevent nonspecific adsorption. A drop of Alexa Fluor 488 anticholera toxin IgG1 (100 μg/mL in 1 × PBS, 1% BSA, 0.25% Tween-20) was applied to the surface and placed inside a humidity chamber (Arrayit Corp., Sunnyvale, CA) for 45 min at room temperature. The unreacted probes were removed by washing with vigorous agitation in 1 × PBS, 1% BSA, 0.25% Tween-20 for 5 min at room temperature, and subsequently rinsed with water.

Surface Hybridization. Agarose DNA patterns on Codelink slides were allowed to react for a minimum of 4 h at 50% humidity and washed with PBS (5 min) under vigorous agitation and rinsed with water to remove residual agarose. These substrates were then passivated with 50 mM ethanolamine in Tris EDTA pH 8 for 1 h room temperature to prevent nonspecific adsorption. For hybridization, the substrate was immersed in a 5′-Cy5-labeled oligonucleotide diluted to 1 μM in 4× saline sodium citrate (SSC, 150 mM NaCl, 15 mM trisodium citrate) containing 0.02% SDS. The substrates were placed in a hybridization oven at 45 °C for 8 h. Unhybridized probes were removed by washing with vigorous agitation in a 1 × SSC with 0.01% SDS solution for 5 min at hybridization temperature, 0.1 × SSC with 0.01% SDS for 5 min at room temp, and subsequent washing in water for 5 min.

Atomic Force Microscopy (AFM). AFM measurements were conducted on a Dimension 3100 scanner with a Nanoscope IV Nanoman controller (Veeco, Santa Barbara, CA) in tapping mode with 512 × 512 data acquisitions and Pointprobe series AFM probes with 42 N/m nominal spring constant (Nanosensors, Neuchatel, Switzerland).

Fluorescence Microscopy. Fluorescent images were obtained with a Carl Zeiss, Axiovert 200 M epifluorescent microscope excited with a mercury lamp filtered to the excitation wavelength of the probed fluorophore (488, 570, 650 nm).

Acknowledgment. C.A.M. acknowledges AFOSR, DARPA/SPAWAR, and NSF for financial support of this research. This work was also partially supported by NanoImpuls/NanoNed, the nanotechnology program of the Dutch Ministry of Economic Affairs (Grant TTF6329).

Supporting Information Available: Microscope images of agarose ink coated AFM tips, AFM image of features before and after washing the agarose matrix, dynamic rheology of bulk agarose inks, and characterization of deposition rate as a function of tricine concentration for CTβ and IgG proteins. This material is available free of charge *via* the Internet at http://pubs.acs.org.

REFERENCES AND NOTES

1. Schena, M.; Shalon, D.; Davis, R. W.; Brown, P. O. Quantitative Monitoring of Gene Expression Patterns with a Complementary DNA Microarray. *Science* **1995**, *270*, 467–470.
2. MacBeath, G.; Schreiber, S. L. Printing Proteins as Microarrays for High-Throughput Function Determination. *Science* **1996**, *289*, 1760–1763.
3. Lockhart, D. J.; Winzeler, E. A. Genomics, Gene Expression, and DNA Arrays. *Nature* **2000**, *405*, 827–836.
4. Christman, K. L.; Enriquez-Rios, V. D.; Maynard, H. D. Nanopatterning Proteins and Peptides. *Soft Matter* **2006**, *2*, 928–939.
5. Lee, K. B.; Park, S. J.; Mirkin, C. A.; Smith, J. C.; Mrksich, M. Protein Nanoarrays Generated By Dip-Pen Nanolithography. *Science* **2002**, *295*, 1702–1705.
6. Vega, R. A.; Maspoch, D.; Salaita, K. W.; Mirkin, C. A. Nanoarrays of Single Virus Particles. *Angew. Chem., Int. Ed.* **2005**, *44*, 6013–6015.
7. Demers, L. M.; Ginger, D. S.; Park, S. J.; Li, Z.; Chung, S.; Mirkin, C. A. Direct Patterning of Modified Oligonucleotides on Metals and Insulators by Dip-Pen Nanolithography. *Science* **2002**, *296*, 1836–1838.
8. Lee, K. B.; Lim, J. H.; Mirkin, C. A. Protein Nanostructures Formed *via* Direct-Write Dip-Pen Nanolithography. *J. Am. Chem. Soc.* **2003**, *125*, 5588–5598.
9. Lim, J.-H.; Ginger, D. S.; Lee, K.-B.; Heo, J.; Nam, J.-M.; Mirkin, C. A. Direct-Write Dip-Pen Nanolithography of Proteins on Modified Silicon Oxide Surfaces. *Angew. Chem., Int. Ed.* **2003**, *42*, 2411–2414.
10. Wu, C.-C.; Xu, H.; Otto, C.; Reinhoudt, D. N.; Lammertink, R. G. H.; Huskens, J.; Subramaniam, V.; Velders, A. H. Porous Multilayer-Coated AFM Tips for Dip-Pen Nanolithography of Proteins. *J. Am. Chem. Soc.* **2009**, *131*, 7526–7527.
11. Tan, Y. H.; Liu, M.; Nolting, B.; Go, J. G.; Gervay-Hague, J.; Liu, G. A Nanoengineering Approach for Investigation and Regulation of Protein Immobilization. *ACS Nano* **2008**, *2*, 2374–2384.
12. Pallandrew, A.; Glinel, K.; Jones, A. M.; Nyste, B. Binary Nanopatterned Surfaces Prepared from Silane Monolayers. *Nano Lett.* **2004**, *4*, 365−371.
13. Renault, J. P.; Bernard, A.; Bietsch, A.; Michel, B.; Bosshard, H. R.; Delamarche, E.; Kreiter, M.; Hecht, B.; Wild, U. P. Fabricating Arrays of Single Protein Molecules on Glass Using Microcontact Printing. *J. Phys. Chem. B* **2003**, *107*, 703–711.
14. Hoff, J. D.; Cheng, L. J.; Maeyhofer, E.; Guo, L. J.; Hung, A. J. *Nano Lett.* **2004**, *4*, 853.
15. Piner, R. D.; Zhu, J.; Xu, F.; Hong, S.; Mirkin, C. A. "Dip-Pen" Nanolithography. *Science* **1999**, *283*, 661–663.
16. Ginger, D. S.; Zhang, H. A.; Mirkin, C. A. The Evolution of Dip-Pen Nanolithography. *Angew. Chem., Int. Ed.* **2004**, *43*, 30–45.
17. Salaita, K.; Wang, Y.; Mirkin, C. A. Applications of Dip-Pen Nanolithography. *Nat. Nanotechnol.* **2007**, *2*, 145–155.
18. Huo, F.; Zheng, Z.; Zheng, G.; Giam, L.; Zhang, H.; Mirkin, C. Polymer Pen Lithography. *Science* **2008**, *321*, 1658–1660.
19. Taha, H.; Marks, R. S.; Gheber, L. A.; Rousso, I.; Newman, J. Protein Printing with an Atomic Force Sensing Nanofountainpen. *Appl. Phys. Lett.* **2003**, *83*, 1041–1043.
20. Braunschweig, A. B.; Senesi, A. J.; Mirkin, C. A. Redox-Activating Dip-Pen Nanolithography (RA-DPN). *J. Am. Chem. Soc.* **2009**, *131*, 922–923.
21. Vega, R. A.; Maspoch, D.; Shen, C. K. F.; Kakkassery, J. J.; Chen, B. J.; Lamb, R. A.; Mirkin, C. A. Functional Antibody Arrays Through Metal Ion-Affinity Templates. *Chembiochem* **2006**, *7*, 1653–1657.
22. Wang, W. M.; Stoltenberg, R. M.; Liu, S.; Bao, Z. Direct Patterning of Gold Nanoparticles Using Dip-Pen Nanolithography. *ACS Nano* **2008**, *2*, 2135–2142.
23. Sekula, S.; Fuchs, J.; Weg-Remers, S.; Nagel, P.; Schuppler, S.; Fragala, J.; Theilacker, N.; Franzreb, M.; Wingren, F.; Ellmark, P.; *et al*. Multiplexed Lipid Dip-Pen Nanolithography on Subcellular Scales for the Templating of Functional Proteins and Cell Culture. *Small* **2008**, *4*, 1785–1793.
24. Normand, V.; Lootens, D.; Amici, E.; Plucknett, K.; Aymard, P. New Insight into Agarose Gel Mechanical Properties. *Biomacromolecules* **2000**, *1*, 730–738.
25. Rees, D. A. Shapely Polysaccharides. *Biochem. J.* **1972**, *126*, 257–273.
26. Mateo, C.; Palomo, J. M.; Fuentes, M.; Betancor, L.; Grazu, V.; Lopez-Gallego, F.; Fernandes-Lafuete, R.; Guisan, J. M. Glyoxyl Agarose: A Fully Inert and Hydrophilic Support for Immobilization and High Stabilization of Proteins. *Enzyme Microbiol. Technol.* **2006**, *39*, 274–280.
27. Luo, Y.; Shoichet, M. S. A Photolabile Hydrogel for Guided Three-Dimensional Cell Growth and Migration. *Nat. Mater.* **2004**, *3*, 249–253.
28. Mayer, M.; Yang, J. C.; Gitlin, I.; Gracias, D. H.; Whitesides, G. M. Micropatterned Agarose Gels for Stamping Arrays of Proteins and Gradients of Proteins. *Proteomics* **2004**, *4*, 2366–2376.
29. Majd, S.; Mayer, M. Hydrogel Stamping of Arrays of Supported Lipid Bilayers with Various Lipid Compositions for the Screening of Drug-Membrane and Protein-Membrane Interactions. *Angew. Chem.* **2005**, *117*, 6697–6700.

30. Watase, M.; Nishinari, K.; Williams, P. A.; Phillips, G. O. Agarose Gels: Effect of Sucrose, Glucose, Urea, and Guanidine Hydrochloride on the Rheological and Thermal Properties. *J. Agric. Food Chem.* **1990**, *38*, 1181–1187.
31. Nishinari, K.; Watase, M. Effects of Polyhydric Alcohols on Thermal and Rheological Properties of Polysaccharide Gels. *Agric. Biol. Chem.* **1987**, *51*, 3238.
32. Normand, V.; Aymard, P.; Lootens, D. L.; Amici, E.; Plucknett, K.; Frith, W. J. Effect of Sucrose on Agarose Gels Mechanical Behaviour. *Carbohydr. Polym.* **2003**, *54*, 83–95.
33. Gamini, A.; Toffanin, R.; Murano, E.; Rizzo, R. Hydrogen-Bonding and Conformation of Agarose in Methyl Sulfoxide and Aqueous Solutions Investigated by ^{1}H and ^{13}C NMR Spectroscopy. *Carbohydr. Res.* **1997**, *304*, 293–302.
34. Singh, T.; Meena, R.; Kumar, A. Effect of Sodium Sulfate on the Gelling Behavior of Agarose and Water Structure Inside the Gel Networks. *J. Phys. Chem. B* **2009**, *113*, 2519–2525.
35. Giam, L. R.; Wang, Y.; Mirkin, C. A. Nanoscale Molecular Transport: The Case of Dip-Pen Nanolithography. *J. Phys. Chem. A* **2009**, *113*, 3779–3782.
36. Wang, H.; Nafday, O. A.; Haaheim, J. R.; Tevaarwerk, E.; Amro, N. A.; Sanedrin, R. G.; Chang, C.; Ren, F.; Pearton, S. J. Toward Conductive Traces: Dip Pen Nanolithography of Silver Nanoparticle-Based Inks. *Appl. Phys. Lett.* **2008**, *93*, 143105-1–3.
37. Jang, J.; Hong, S.; Schatz, G. C.; Ratner, M. A. Self-Assembly of Ink Molecules in Dip-Pen Nanolithography: A Diffusion Model. *J. Chem. Phys.* **2001**, *115*, 2721–2729.
38. Ivanisevica, A.; Mirkin, C. A. "Dip-Pen" Nanolithography on Semiconductor Surfaces. *J. Am. Chem. Soc.* **2001**, *123*, 7887–7889.
39. Beaucage, S. L.; Caruthers, M. H. Deoxynucleoside Phosphoramidites—A New Class of Key Intermediates for Deoxypolynucleotide Synthesis. *Tetrahedron Lett.* **1981**, *22*, 1859–1862.